Extracellular Matrix of Glioblastoma Inhibits Polarization and Transmigration of T Cells: The Role of Tenascin-C in Immune Suppression

Jyun-Yuan Huang, Yu-Jung Cheng, Yu-Ping Lin, Huan-Ching Lin, Chung-Chen Su, Rudy Juliano and Bei-Chang Yang

J Immunol 2010;185;1450-1459; Prepublished online 9 July 2010;
doi:10.4049/jimmunol.0901352
http://www.jimmunol.org/content/185/3/1450

The Journal of Immunology is published twice each month by The American Association of Immunologists, Inc., 9650 Rockville Pike, Bethesda, MD 20814-3994.

Print ISSN: 0022-1767 Online ISSN: 1550-6606.

Extracellular Matrix of Glioblastoma Inhibits Polarization and Transmigration of T Cells: The Role of Tenascin-C in Immune Suppression

Jyun-Yuan Huang,* Yu-Jung Cheng,† Yu-Ping Lin,* Huan-Ching Lin,* Chung-Chen Su,* Rudy Juliano,‡ and Bei-Chang Yang*,†,§

Dense accumulations of T cells are often found in peritumoral areas, which reduce the efficiency of contact-dependent lysis of tumor cells. We demonstrate in this study that the extracellular matrix (ECM) produced by tumors can directly regulate T cell migration. The transmigration rate of several T cells including peripheral blood primary T cell, Jurkat, and Molt-4 measured for glioma cells or glioma ECM was consistently low. Jurkat cells showed reduced amoeba-like shape formation and delayed ERK activation when they were in contact with monolayers or ECM of glioma cells as compared with those in contact with HepG2 and MCF-7 cells. Phospho-ERK was located at the leading edge of migrating Jurkat cells. Glioma cells, but not MCF-7 and HepG2 cells, expressed tenascin-C. Knocking down the tenascin-C gene using the short hairpin RNA strategy converted glioma cells to a transmigration-permissive phenotype for Jurkat cells regarding ERK activation, transmigration, and amoeba-like shape formation. In addition, exogenous tenascin-C protein reduced the amoeba-like shape formation and transmigration of Jurkat cells through MCF-7 and HepG2 cell monolayers. A high level of tenascin-C was visualized immunohistochemically in glioma tumor tissues. $CD3^+$ T cells were detected in the boundary tumor area and stained strongly positive for tenascin-C. In summary, glioma cells can actively paralyze T cell migration by the expression of tenascin-C, representing a novel immune suppressive mechanism achieved through tumor ECM. ***The Journal of Immunology*****, 2010, 185: 1450–1459.**

Tumor-specific immune responses are detectable in patients with cancer (1). The infiltration of immune cells into the tumor region is a promising indicator of better prognosis for a variety of cancers (2–4). However, tumor masses are usually surrounded by a basal membrane-like structure composed of distinctive extracellular matrix (ECM) components that physically separate tumor cells from other tissue compartments (5, 6). Isoforms of ECMs are uniquely expressed in different tissues and tumors. ECM acts not only as a protein scaffold to support tissues and organ assemblies, but also transmits signals through cell-surface receptors to regulate cell adhesion, migration, proliferation, and differentiation (7, 8). For tumor-infiltrating T cells, the PI3K/Akt pathway initiated upon contact with tumor cells through β-integrins suppresses the Fas-mediated apoptosis in T cells (9).

During the course of infiltration, immune cells have to migrate out of blood vessels and travel some distance to get into the tumor site. There, they encounter a distinct environment composed of various ECM components, which are very different from those of the bloodstream. In addition, these immune cells have to penetrate the ECM-rich capsule surrounding tumor masses. Activated T cells adhere strongly to type IV collagen but weakly to type I collagen, indicating that specific ECM components have a role in cell infiltration (10). Marked lymphocyte infiltration occurs outside the collagen I/II-rich capsule of hepatocellular carcinoma or surrounding compressed hepatocytes near the capsule (11). However, the impact of tumor ECM on the infiltration of NK and T cells has been disputed. On one hand, tight basal membrane-like structures found around the tumor masses potentially prevent direct contact of NK cells or T cells with tumor nests (12, 13). On the other hand, the infiltration of immune cells requires the presence of certain tumor ECM molecules. For instance, activated NK and T cell infiltration is observed in loose metastatic melanoma masses that contain high amounts of ECM components including laminin-1, fibronectin, and collagen (14, 15). As in local hepatoma in the liver, the stroma of colorectal hepatic metastases is heavily infiltrated by lymphocytes that colocalize with vitronectin, whereas the tumors lacking vitronectin are devoid of lymphocytes (16).

Migrating lymphocytes are polarized, in which migration-controlling kinases, including PI3K and AKT, are recruited to the leading front of migrating cells and may facilitate actin polymerization (17, 18). Preventing the adhesion of cells blocks the mitogen-induced activation of the canonical MAPK, which is important for T cell adhesion and migration (19–21). Although individual matrix proteins such as fibronectin and laminin have been shown to regulate ERK/MAPKs, the overall signaling for T cell migration triggered by tumor ECM with its distinctive protein components is still poorly understood.

*Institute of Basic Medical Sciences, †Department of Microbiology and Immunology, College of Medicine, and §Center for Gene Regulation and Signal Transduction Research, National Cheng Kung University, Tainan, Taiwan; and ‡Department of Pharmacology, School of Medicine, University of North Carolina, Chapel Hill, NC 27599

Received for publication April 30, 2009. Accepted for publication April 30, 2010.

This work was supported by Grants NSC96-2320-B-006-021-MY3 and NSC95-2320-B-006-003 from the National Science Council, Taiwan, Republic of China (to B.-C.Y.) and by Grant DOH99-TD-C-111-003 to the Comprehensive Cancer Center in Southern Taiwan.

Address correspondence and reprint requests to Dr. Bei-Chang Yang, Department of Microbiology and Immunology, College of Medicine, National Cheng Kung University, Tainan, Taiwan. E-mail address: y1357@mail.ncku.edu.tw

The online version of this article contains supplemental material.

Abbreviations used in this paper: COL IV, collagen IV; ECM, extracellular matrix; EGFP, enhanced GFP; F, forward; FAK, focal adhesion kinase; FN, fibronectin; LAM, laminin-γ1; pAKT, phosphorylated AKT; pCREB, phosphorylated CREB; pERK, phosphorylated ERK; PKA, protein kinase A; R, reverse; sh, short hairpin; TN-C, tenascin-C.

www.jimmunol.org/cgi/doi/10.4049/jimmunol.0901352

To understand the impact of tumor ECM on T cell migration, we investigated the migration behaviors of T cells through tumor cell monolayers and extracted tumor ECM. We found that the cell monolayer and ECM of glioblastoma inhibited the transmigration of T cells. Confocal imaging and time-lapse videomicroscopy showed that the low migration rate of Jurkat cells correlated with delayed ERK activation and reduced lamellipodia formation. Furthermore, we demonstrated that tenascin-C expressed on glioblastoma cells inhibited the migration of T cells, providing a possible mechanism for the immune suppression found in brain tumors.

Materials and Methods

Reagents and Abs

Kinase inhibitors for MEK (U0126) and PI3K (LY294002) were purchased from Calbiochem (La Jolla, CA). Collage IV, fibronectin, and goat polyclonal anti-human CD3 Ab were obtained from Santa Cruz Biotechnology (Santa Cruz, CA). Protein kinase A (PKA) inhibitor (H-89), laminin, phalloidin-FITC (P5282), and puromycin were purchased from Sigma-Aldrich (St. Louis, MO). Short hairpin (sh)RNA interference pLKO.1-shTNC for tenascin-C was obtained from the National RNAi Core Facility of Taiwan (Taipei, Taiwan). Plasmid pEGFP-N1 was purchased from Clontech Laboratories (Palo, Alto, CA). Rabbit Abs for ERK and phospho-ERK were obtained from Cell Signaling Technology (Beverly, MA). Rabbit Abs for CREB and phospho-CREB were purchased from Upstate Biotechnology (Lake Placid, NY). Mouse anti-human integrin β1- and β2-blocking Abs and human tenascin-C were obtained from Chemicon International (Temecula, CA). RGD peptide was kindly provided by Dr. Woei-Jer Chuang (National Cheng Kung University, Tainan, Taiwan). Donkey anti-goat Ab (Alexa Fluor 488 conjugated), goat anti-rabbit Ab (Alexa Fluor 488 conjugated), donkey anti-mouse Ab (Alexa Fluor 594 conjugated), and Hoechst 33258 nucleic acid stain were purchased from Invitrogen Life Technologies (Grand Island, NY). Functional grade purified anti-human CD3 and CD28 Abs were obtained from eBioscience (San Diego, CA). Dako Ab diluent and HRP-conjugated goat anti-rabbit IgG Ab were purchased from DakoCytomation (Glostrup, Denmark). Mouse monoclonal anti-human tenascin-C Ab was obtained from Abcam (Cambridge, U.K.).

Cell cultures and transfections

Human T cell leukemia cell lines Jurkat (E6-1) and Molt-4, breast carcinoma cell line MCF-7, glioblastoma cell lines U-118MG, U-373MG, and U-87MG, and hepatocellular carcinoma cell line HepG2 were obtained from the American Type Culture Collection (Manassas, VA). Human PBMCs were prepared using Ficoll-Hypaque Plus (Amersham Biosciences, Uppsala, Sweden) density gradient centrifugation. $CD3^+$ T cells in PBMCs were further purified by passing through a sterile column of nylon wool. Jurkat, Molt-4, and primary T cells were cultured in RPMI 1640 medium (Life Technologies) supplemented with 10% FBS and 1% antibiotic-antimycotic. Primary T cells were activated by CD3 plus CD28 Abs (5 μg/ml) for 3 d. MCF-7, U-87MG, U-118MG, U-373MG, and HepG2 were cultured in DMEM medium (Invitrogen, Carlsbad, CA) supplemented with 10% FBS, 2 mM L-glutamine, and 1% antibiotic-antimycotic. Cells were grown at 37°C in an air/5% CO_2 atmosphere at constant humidity. We transfected the enhanced GFP (EGFP) gene into Jurkat cells. EGFP-expressing Jurkat cells emit green light under fluorescent microscopy and can be unambiguously identified among a mixed-cell population. Jurkat cells expressing EGFP, noted as Jurkat (N1) cells, were established by transfecting the parental E6-1 cells with plasmid pEGFP-N1 according to the manufacturer's protocol for MircoPorator MP-100 (Nano-EnTek, Seoul, Korea). To knock down the tenascin-C gene, U-118MG cells were transfected with plasmid pLKO.1-shTNC, noted as U-118MG (TNCshRNA) cells, or a control plasmid according to the manufacturer's protocol for Lipofectamine 2000 (Invitrogen).

Transmigration assay

A transmigration assay was performed using a 24-well transwell system (6.5-mm diameter, 5-μm pores; Costar, Cambridge, MA). To study the effect of ECM components, the insert membrane of the transwell was coated with collagen IV, fibronectin, laminin, or BSA at concentrations indicated. For transmigration through tumor cell monolayers, MCF-7, U-87MG, U-118MG, U-373MG, or HepG2 cells were cultured on the insert membrane at 4×10^4 cells/well for 2 d to confluence. For tumor cell matrix experiments, the confluent tumor cell monolayers were extracted with 0.5% Triton X-100, followed by one rinse with 0.1 M NH_4OH and three rinses with PBS (22), and then washed twice with RPMI 1640 containing 1% FBS. A total of $\sim 5 \times 10^5$ (100 μl/well) T cells in 1% FBS/RPMI 1640 were loaded into the upper well. RPMI 1640 containing 10% FBS was added to the lower wells (600 μl/well). Cells that migrated to the lower wells after 4 h of incubation in 5% CO_2 at 37°C were counted. For inhibition experiments, T cells were suspended in human tenascin-C protein solution (10 μg/ml) or treated for 30 min with anti-human integrin-blocking Abs (10 μg/ml), RGD peptide (5 μM), U0126 (25 μM), LY294002 (25 μM), or H-89 (10 nM) before being subjected to the transmigration assay.

Morphological observation and confocal microscopy

Jurkat cells were suspended in 1% FBS RPMI 1640 and added directly onto the cell monolayer or matrix of MCF-7, U-118MG, or HepG2. After 1 h of incubation, cell morphology was observed by fluorescent microscopy or time-lapse microscopy. Cell images were captured at 30-s intervals. For protein staining, Jurkat cells adhering to the cell matrix were fixed with 4% paraformadehyde for 15 min and permeabilized with 0.1% Triton X-100 for 10 min. F-actin was stained by FITC-conjugated phalloidin (0.5 μM) for 40 min. Localization of ERK at the lamellipodia was observed by confocal microscopy. Jurkat cells attached to the tumor matrix were washed twice with PBS, fixed in 4% paraformaldehyde for 30 min, washed twice with PBS, then treated with a blocking solution containing 2% FBS and 1% BSA in PBS for 1 h. Cells were incubated overnight with Abs recognizing phospho-ERK. After washing with PBS, the cells were incubated with goat anti-rabbit IgG (Alexa Fluor 488 conjugated) and FITC-conjugated phalloidin. Images were taken using a Leica TCS SPII confocal microscope (Leica Microsystems, Nussloch, Germany) with excitation set at 488 nm.

RT-PCR

Total RNA was extracted using TRIzol reagent (Invitrogen) according to the manufacturer's instructions. Reverse transcription was performed at 37°C for 60 min in a 20-μl reaction containing 2 μg RNA, 500 ng oligo(dT) primers, 4 μl 5× RT buffer (250 mM Tris-HCl [pH 8.3], 375 mM KCl, 15 mM $MgCl_2$, and 50 mM DTT), 0.5 μl of 40 mM 2′-deoxynucleoside 5′-triphosphate, 0.5 μl of 200 U/μl RNase inhibitor (Promega, Madison, WI), 3.5 μl diethyl pyrocarbonate-treated water, and 1 μl of 200 U/μl M-MLV reverse transcriptase (Promega, Madison, WI). The oligonucleotide primers used are listed in Table I (23–26). PCR cycles were carried out on a DNA thermal cycler (Hybaid Omnigene, Middlesex, U.K.). Human β-actin served as a quantitative control in PCR. PCR products were fractionated with agarose, stained with ethidium bromide, and visualized under UV light.

Western blot

Jurkat cells were collected and lysed in a buffer consisting of 250 mM Tris-HCl (pH 7.5), 150 mM NaCl, 1 mM EDTA, 1 mM EGTA, 1% Triton X-100, 1 mM Na_3VO_4, 1 mM PMSF, and a protease inhibitors mixture containing 500 μM 4-(2-aminoethyl)-benzenesulfonyl fluoride, 1 μg/ml aprotinin, 1 μM E-64, 500 μM EDTA, and 1 μM leupeptin (Calbiochem). Proteins were separated by 12% SDS-PAGE and transferred to the polyvinylidene difluoride membrane. The membrane was then incubated with blocking solution (5% BSA in 0.15% TBST) for 1 h, followed by incubation with the primary Ab at 4°C overnight, then probed with HRP-conjugated goat anti-rabbit IgG Ab. Immunocomplexes were made visible by fluorography using an ECL detection kit (Amersham Biosciences).

Immunofluorescent stain

Glioma tissues were obtained from the National Core Facilities of the National Research Program for Genomic Medicine-Tumor Tissue Bank in Southern Taiwan. Five-micrometer serial tissue sections were prepared and mounted on slides. After treating with ice-cold acetone for 2 min, the slides

Table I. *The oligonucleotide primers used in this study*

Collagen type IV	F: 5′-GGGCTACCTGGAGAAAAAGG-3′
	R: 5′-TCCTGGAGAGCCACCAATAC-3′
Fibronectin	F: 5′-AAGGTTCGGGAAGAGGTTGT-3′
	R: 5′-TGGCACCGAGATATTCCTTC-3′
Laminin γ1	F: 5′-CACTGTGAGAGGTGCCGAGAGAAC-3′
	R: 5′-CATCCTGCTTCAGTGAGAGAATGG-3′
Tenascin-C	F: 5′-GTGAAGGCATCCACTGAACAAGC-3′
	R: 5′-TTGTGCTGAAGTCCTGAGTGACC-3′
β-actin	F: 5′-GATGAGATTGGCATGGCTTT-3′
	R: 5′-CACCTTCACCGTTCCAGTTT-3′

F, forward; R, reverse.

were incubated with PBS containing 10% FBS at room temperature for 30 min. The slides were then incubated overnight at 4°C with a mouse anti-human tenascin-C mAb and a goat polyclonal anti-human CD3 Ab diluted 1:100 in Ab diluent. Secondary hybridization was done using a donkey anti-goat Ab (Alexa Fluor 488 conjugated) and a rabbit anti-mouse Ab (Alexa Fluor 594 conjugated). Cell nuclei were stained with Hoechst 33258 (Life Technologies). The tenascin-C– and $CD3^+$-labeled cells, showing red and green, respectively, were observed with a fluorescent microscope system (Olympus, Tokyo, Japan).

Statistical analysis

The data were obtained from at least three independent experiments and are expressed as mean ± SEM. The differences between groups were analyzed using the Student *t* test, and $p < 0.05$ was considered significant.

Results

Interaction of ECM and integrins plays a role in the transmigration of T cells

Jurkat and Molt-4 cells easily transmigrated across the monolayers of MCF-7 and HepG2 cells grown on transwell filters toward nutrition. At 4 h, ~10–20% of Jurkat and Molt-4 cells transmigrated across the cell monolayers of MCF-7 and HepG2. By contrast, <5% of Jurkat and Molt-4 cells transmigrated across the cell monolayers of U-373MG, U-87MG, and U-118MG (Fig. 1*A*, *upper panels*). Similarly, transmigration of nonactivated primary T cells through the cell monolayers of U-87MG, U-118MG, and U-373MG was less than that through the cell monolayers of MCF-7 and HepG2. However,

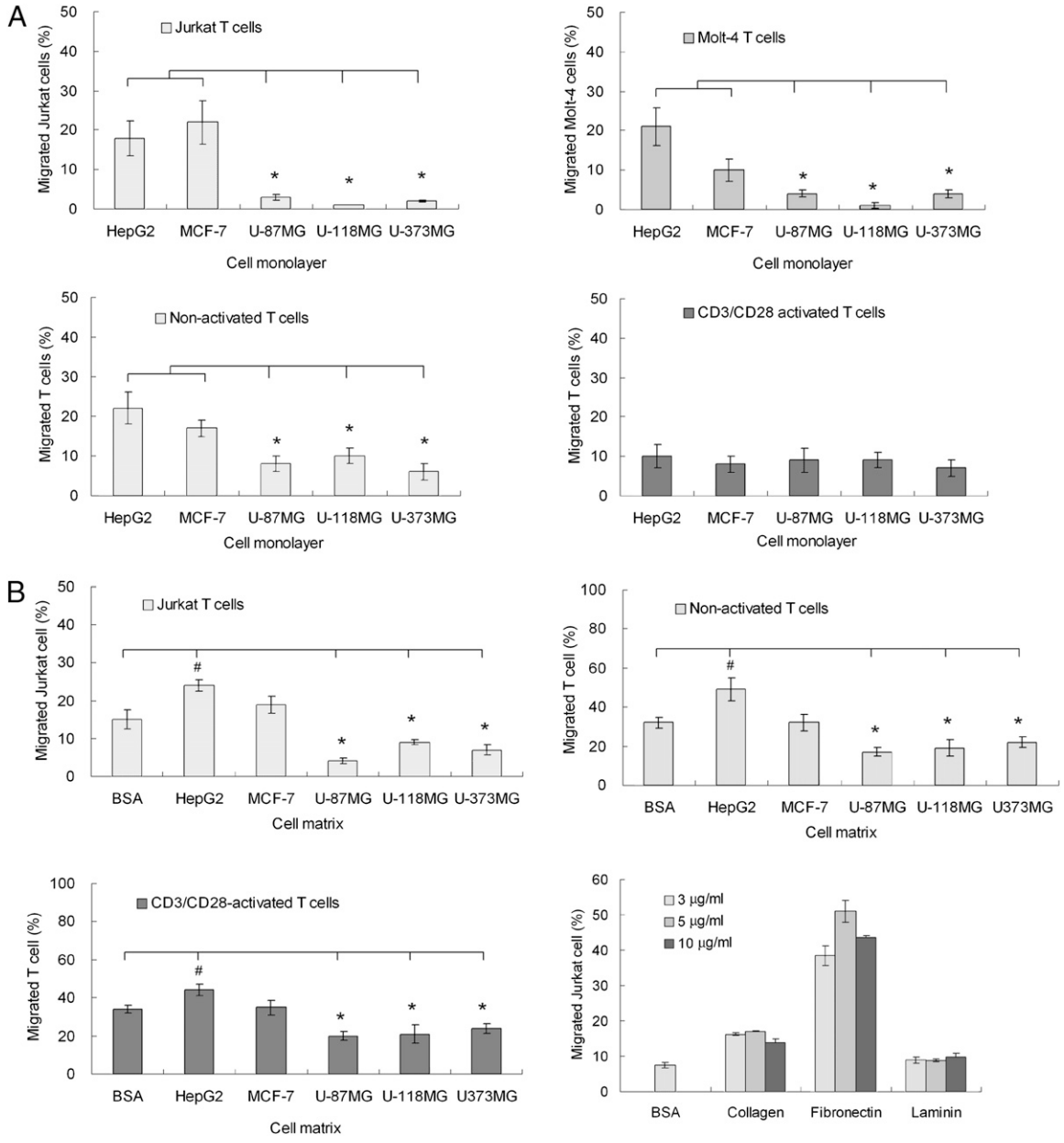

FIGURE 1. The transmigrations of T cells through the tumor monolayers and ECM. MCF-7, U-87MG, U-118MG, U-373MG, and HepG2 cells were grown on the insert membrane of a transwell unit. *A*, Jurkat, Molt-4, or primary T cells suspended in 1% FBS/RPMI 1640 that transmigrated through the cell monolayer to the lower well containing 10% FBS/RPMI 1640 were counted at 4 h. Primary T cells were activated by CD3 plus CD28 Abs (5 μg/ml) for 3 d before being subjected to transmigration experiments. The transmigration rates of T cells through glioma cell monolayers were compared with those through MCF-7 or HepG2 cell monolayers. $*p < 0.05$. *B*, The transmigrations of Jurkat cells and nonactivated and CD3/CD28-activated T cells across tumor ECM layers in 4 h were compared ($^{\#}p < 0.05$, higher than BSA control; $*p < 0.05$, lower than BSA control). Medium containing 10% FBS/RPMI 1640 served as the attractant. ECMs were made of MCF-7, U-87MG, U-118MG, U-373MG, or HepG2 monolayers by extraction with 0.5% Triton X-100, as described in *Materials and Methods*. BSA-coated (10 μg/ml) membrane served as control. Transmigration of Jurkat cells through membranes coated with fibronectin, collagen, and laminin (3, 5, and 10 μg/ml) were compared.

CD3/CD28-activated T cells tended to adhere to tumor monolayers and showed reduced transmigration through the tumor monolayer than nonactivated T cells (Fig. 1*A*, *lower panels*). Further, we prepared tumor ECMs by extracting monolayers of MCF-7, U-87MG, U-118MG, U-373MG, and HepG2 with 0.5% Triton X-100 and 0.1 M NH_4OH, as described in *Materials and Methods*. Jurkat cells moved across the insert membrane coated with ECM of MCF-7 cells to a level similar to that of the BSA-coated control. ECM of HepG2 cells stimulated Jurkat cell transmigration. By contrast, the transmigration rates of Jurkat cells through ECM of U-373MG, U-87MG, and U-118MG cells were only ~40% of BSA control (Fig. 1*B*, *left upper panel*). Similarly, nonactivated and CD3/CD28-activated T cells showed a low transmigration rate across the glioma ECM (Fig. 1*B*, *right upper panel* and *left lower panel*). In addition, we found that a higher transmigration rate of Jurkat cells was observed for collagen and fibronectin, about two and five times higher than that of the BSA control, respectively. Laminin did not enhance the transmigration rate of Jurkat cells (Fig. 1*B*, *right lower panel*).

Adhesion and morphological change of Jurkat cells

When Jurkat cells were in contact with HepG2 and U-118MG cells, a strong adhesion was quickly established, and many Jurkat cells

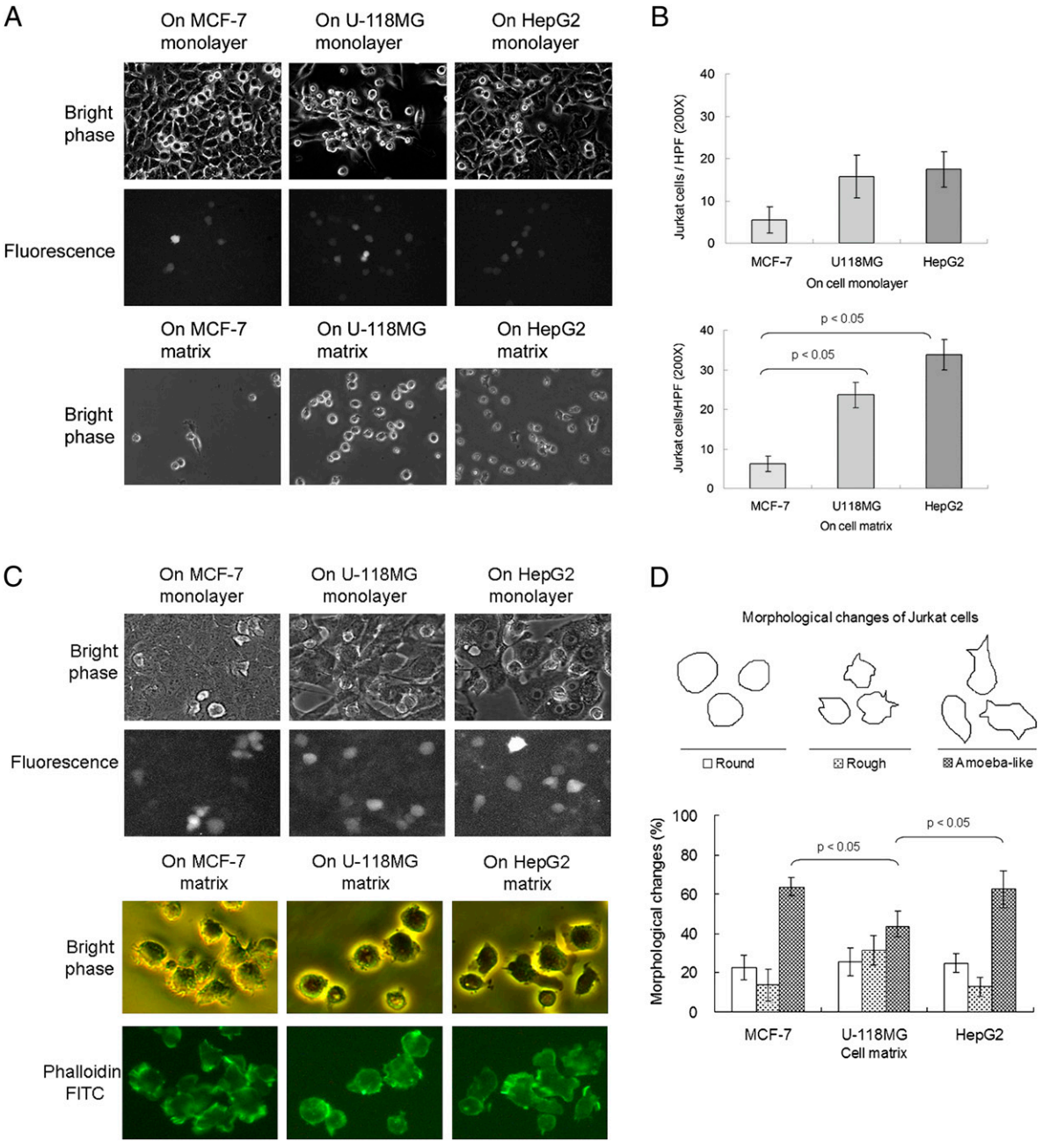

FIGURE 2. Adhesion and morphological change of Jurkat cells on the monolayers or ECM of tumor cells. *A*, Jurkat cells expressing EGFP were added onto cell monolayers of confluent MCF-7, U-118MG, and HepG2 cells grown on 4-cm culture dishes or incubated on ECM of tumors extracted by Triton X-100. After 1 h of coculture, the cell suspension was removed. The culture plate was gently washed once with PBS. Representative images of Jurkat cells in contact with tumor cell monolayers and Triton-extracted tumor matrix (original magnification ×200). *B*, Adherent Jurkat cells were counted in 10 randomly selected observations using a microscope. The mean ± SEM obtained from three independent experiments are shown. *C*, Jurkat cells on tumor cell monolayers or ECM were observed at a high magnification (×200) using time-lapse microscopy. *D*, Images were recorded every 30 s for 1 h. Based on the cell shape, Jurkat cells were classified as round, rough, and amoeba-like. The percentages of each cell type after 1 h incubation were calculated. F-actin was stained by FITC-conjugated phalloidin (*C, lower panel*; original magnification ×400).

were still attached to tumor cell monolayers after gentle shaking and washing with PBS. Jurkat cells sitting on the MCF-7 cell monolayer were easily shaken off (Fig. 2*A*, *upper panels*). Similarly, Jurkat cells adhered tightly to the ECM of HepG2 and U-118MG cells, but loosely to the ECM of MCF-7 cells (Fig. 2*A*, *lower panel*). Under the same shaking conditions, the number of Jurkat cells staying on HepG2 and U-118MG cell monolayers or ECM was about five times more than that on the MCF-7 cell monolayer or ECM (Fig. 2*B*).

Jurkat cell morphology started to change when the cells adhered onto the tumor cell monolayer and ECM (Fig. 2*C*), and it can be classified into three distinct groups based on the cell shape: round, rough, and amoeba-like (Fig. 2*D*). We used a time-lapse microscope to study the dynamic change of cell morphology (Supplemental Videos 1–3). Jurkat cells with a round shape did not actively move during the observation time period. Rough Jurkat cells showed short podia-like protrusions, which retracted frequently. Amoeba-like cells, very active in migration, showed a polarized body with full extension of filopodia and lamellipodia at the leading edge. We occasionally observed that some Jurkat cells with the amoeba-like shape squeezed into the cell–cell junction of the tumor monolayer and crawled underneath. To correlate the morphology with cell migration, we stained with F-actin (Fig. 2*C*, *lower panels*). F-actin colocalized with lamellipodia at the leading edge of polarized Jurkat cells on the ECM of MCF-7 and HepG2 cells.

By counting the distinct shapes of Jurkat cells, we found that cell contact induced morphological changes to the Jurkat cells in a tumor-specific manner. Although Jurkat cells strongly adhered to the U-118MG cell monolayer, they tended to stay round in shape and were relatively less amoeba-like. In contrast, Jurkat cells stably adhered onto the HepG2 cell monolayer, yet they quickly became amoeba-like. Although Jurkat cells only loosely adhered to the MCF-7 cell monolayer, most of them became amoeba-like in 1 h. Jurkat cells showed similar behavior in response to tumor ECM (Fig. 2*C*, *upper panels*). Tumor ECMs induced similar morphological changes in Jurkat cells. ECM extracted from MCF-7 and HepG2 cells were more effective in inducing Jurkat cells to become an amoeba-like shape than ECM from U-118MG cells. When plated on a culture dish coated with the ECM of HepG2 and MCF-7 cells, 20% of the Jurkat cells were round, 10% were rough, and 70% were amoeba-like. Jurkat cells on the ECM from U-118MG cells were relatively less mobile and different in cell shape; ~20% were round, 40% were rough, and 40% were amoeba-like (Fig. 2*D*).

Tumor cells express different levels of tenascin-C, collagen IV, laminin-γ1, and fibronectin

To distinguish the ECM composition of tumor cells, we analyzed the expressions of collagen, fibronectin, laminin, and tenascin-C (Fig. 3*A*; primers see Table I). The transcripts of fibronectin and laminin-γ1 were detected in MCF-7, HepG2, U-87MG, U-118MG,

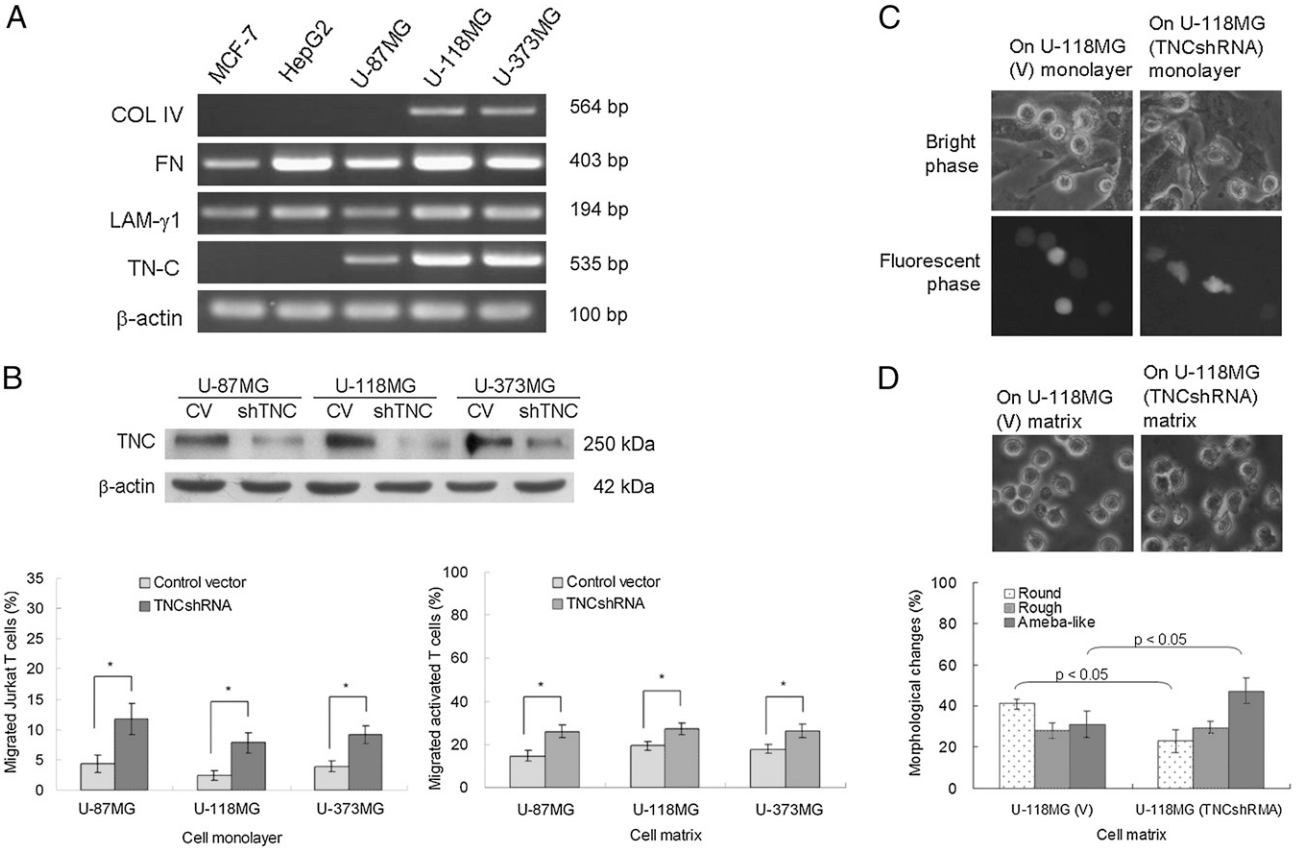

FIGURE 3. Expression of tenascin-C in tumor cells. *A*, The transcripts of COL IV, FN, LAM, and TN-C were detected by RT-PCR with primer sets as described in *Materials and Methods*. *B*, To knock down the expression of tenascin-C, U-87MG, U-118MG, and U-373MG cells were transfected with plasmid pLKO.1-shTNC. Reduced expression of tenascin-C is confirmed by Western blot analysis. ECM layers were made of glioma cell monolayers by extraction with 0.5% Triton X-100 as described in *Materials and Methods*. Medium containing 10% FBS/RPMI 1640 served as the attractant. The transmigrations of Jurkat cells and CD3/CD28-activated T cells through the tumor monolayer and ECM in 4 h, respectively, were measured. Morphology of Jurkat cells was observed postcontact with the U-118MG (TNCshRNA) monolayer (*C*) and ECM (*D*) for 1 h using time-lapse microscopy (original magnification ×200). Representative images are shown. The percentage of each cell type was calculated. $*p < 0.05$. COL IV, collagen IV; FN, fibronectin; LAM, laminin-γ1; TN-C, tenascin-C.

and U-373MG. Collagen IV transcripts were detected in U-118MG and U-373MG cells, but not in MCF-7, HepG2, and U-87MG cells. Tenascin-C transcripts were detected in U-87MG, U-118MG, and U-373MG cells, but not in MCF-7 and HepG2 cells. In cell culture, U-87MG, U-118MG, and U-373MG showed strong stain intensities for tenascin-C, not only in the cell body but also in extracellular space (Supplemental Fig. 1). It has been shown that tenascin-C, but not collagen IV, exhibits the immune-suppression effect and suppresses chemotaxis of human monocytes and neutrophils (27, 28). Therefore, we specifically knocked down the expression of tenascin-C in U-87MG, U-118MG, and U-373MG cells using the shRNA strategy (Fig. 3*B*, *upper panel*). Suppression of tenascin-C did not alter the morphology of these glioma cells. Transmigrations of Jurkat cells and CD3/CD28 activated T cells through the monolayer and ECM of U87MG (TNCshRNA), U-118MG (TNCshRNA), and U373MG (TNCshRNA) cells, respectively, were significantly increased as compared with that obtained from the control groups (Fig. 3*B*, *lower panels*). This finding of a markedly elevated transmigration rate of Jurkat cells toward U-118MG (TNCshRNA) cells is consistent with an increase in the amoeba-like cell population (Fig. 3*C*). Jurkat cells still adhered stably to the U-118MG (TNCshRNA) cell monolayer, but many of them started to become amoeba-like. Similarly, Jurkat cells underwent morphological changes on the tumor matrix extracted from U-118MG (TNCshRNA) cells. Jurkat cells with an amoeba-like shape increased ~2-fold on the U-118MG (TNCshRNA) cell matrix as compared with those on the U-118MG (V) cell matrix (Fig. 3*D*). We then suspended Jurkat cells in human tenascin-C solution and performed the transmigration assay. We found that there was a 2-fold reduction in the transmigration rate of Jurkat cells through MCF-7 and HepG2 cell monolayers in the presence of additional human tenascin-C at 10 and 5 μg/ml, but not at 2.5 μg/ml (Fig. 4*A*). The exogenous tenascin-C also significantly reduced the transmigration rate of CD3/CD28 activated T cells through ECM of MCF-7 and HepG2 cells (Fig. 4*B*). Human tenascin-C protein also decreased the formation of amoeba-like Jurkat cells on the MCF-7 and HepG2 cell monolayers (Fig. 4*C*).

The effects of blocking Abs and RDG peptide on the transmigration

Treating Jurkat T cells with integrin β1- and β2-blocking Abs or RGD peptide reduced the transmigration rates through the MCF-7 and HepG2 cell monolayers by ~20–40%, but did not affect that through the U-118MG cell monolayer (Fig. 5*A*). The blocking anti–tenascin-C Ab (BC-24) showed no effect on the transmigration of Jurkat T cells through glioma cell monolayers (Fig. 5*B*).

The expression of tenascin-C in glioma tissue correlates with CD3$^+$ T cell distribution

The effect of tenascin-C on T cell infiltration was established in vivo by immunofluorescent stain (Fig. 6). Glioma cells were stained positive with tenascin-C. An accumulation of tenascin-C around blood vessels in all glioblastoma tissues has been reported (29), and, in support of this, we found that many CD3-positive cells accumulated in the blood vessels stained strongly with tenascin-C. Few CD3-positive cells transmigrated into brain tumor tissue. In addition, tenascin-C inhibited the LPS-induced in vivo migration of leukocytes into the mouse air pouch model (Supplemental Fig. 2).

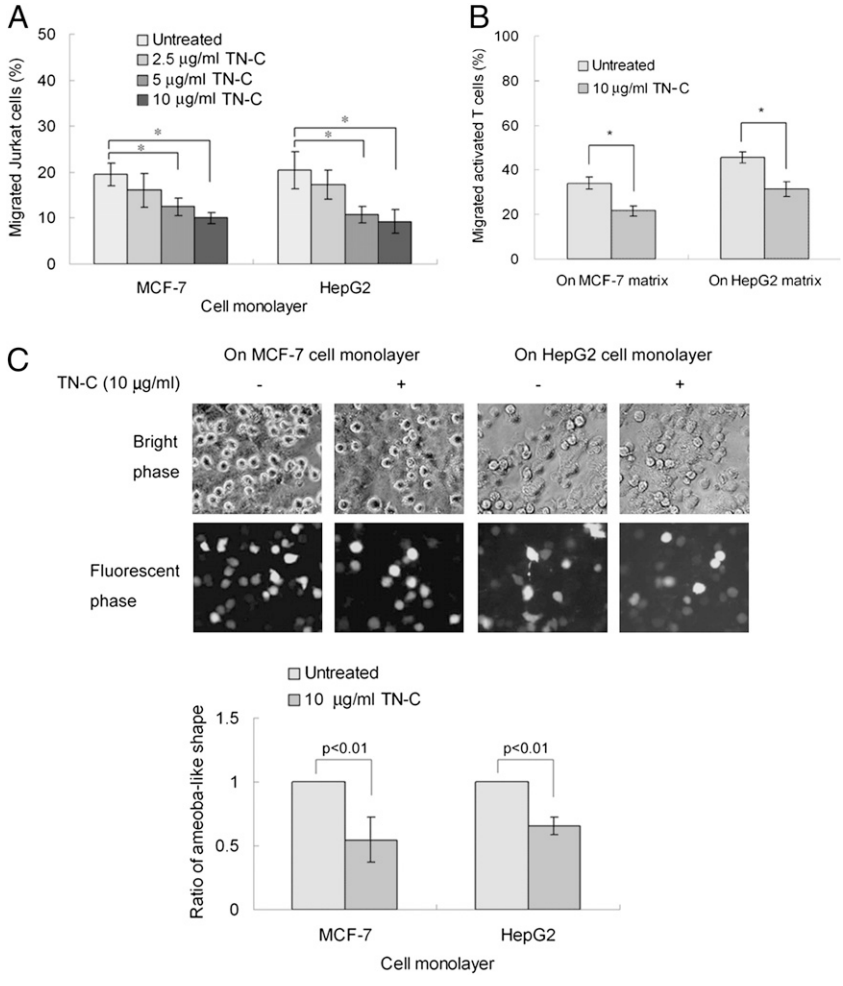

FIGURE 4. The effect of tenascin-C on the transmigration and morphological changes of Jurkat cells. *A*, The transmigrations of Jurkat cells through MCF-7 and HepG2 cell monolayers in the presence of human tenascin-C solution (2.5, 5, 10 μg/ml) in 4 h were measured. *B*, CD3/CD28-activated T cells suspended in human tenascin-C solution (10 μg/ml) were tested. Medium containing 10% FBS/RPMI 1640 served as attractant. *C*, Jurkat (N1) cells suspended in tenascin-C (10 μg/ml) were added onto monolayers of MCF-7 and HepG2 cells grown on a 96-well culture plate. After 1 h incubation, the amoeba-like shape cells were counted for Jurkat cells attached to MCF-7 and HepG2 cell monolayers in 10 randomly selected observations using a fluorescent microscope (original magnification ×200). $*p < 0.05$.

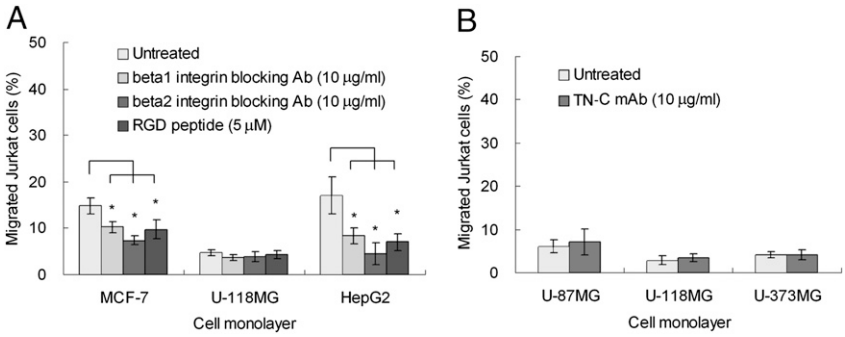

FIGURE 5. The effects of blocking Abs and RDG peptide on the transmigration. *A*, To block the integrin-ECM interaction, Jurkat cells were pretreated with integrin β1- and β2-blocking Abs (10 μg/ml) or RGD peptide (5 μM) for 30 min. Transmigration of Jurkat cells through the MCF-7, U-118MG, and HepG2 cell monolayers in response to nutrition attraction was measured in the presence of blocking Abs. *B*, Transmigration of Jurkat cells through the U-87MG, U-118MG, and U-373MG cell monolayers in response to nutrition attraction was measured in the presence of blocking Ab (BC-24) (10 μg/ml). The mean ± SEM obtained from three independent experiments is shown. $*p < 0.05$.

Tumor contact activates focal adhesion kinase, ERK, and PKA activities in Jurkat cells, which are required for the transmigration of these cells

Given the marked effect of the tumor cell matrix on the morphology of Jurkat T cells, we concerned ourselves with the nature of the signaling proteins that mediate this event. Activation of focal adhesion kinase (FAK) has been demonstrated in cell adhesion at a very early stage. FAK phosphorylation in Jurkat cells was induced in 10 min by contact with MCF-7, U118MG, and HepG2 cells (Fig. 7*A*). We further examined the migration-related kinases including ERK, PKA, and PI3K activities of Jurkat cells cultured on the tumor cell monolayers (Fig. 7*B*, *upper panel*) and tumor ECM-coated plates (Fig. 7*B*, *lower panel*). ERK activity of Jurkat cells was quickly stimulated by the ECM of MCF-7 cells. Specifically, the phosphorylation of ERK in Jurkat cells was strongly upregulated within 10 min of contact with the MCF-7 monolayer, which was sustained for >60 min. Jurkat cells in contact with the U-118MG monolayer showed a delayed induction of ERK phosphorylation that increased slightly at 60 min postcontact. Similarly, the phosphorylation of ERK was mild and slow in Jurkat cells on the ECM of U-118MG cells (Fig. 7*B*, *lower panel*). In contrast to ERK, Jurkat cells have a high intrinsic level of PI3K activity, shown by a high level of AKT phosphorylation. Jurkat cells exposed to ECM from MCF-7 and U-118MG cells did not change this status. Both the tumor ECMs of MCF-7 and U-118MG cells significantly increased the phosphorylation of CREB in Jurkat cells. Direct contact with the tumor monolayers of MCF-7 and U-118MG cells also stimulated similar phosphorylation of CREB in Jurkat cells.

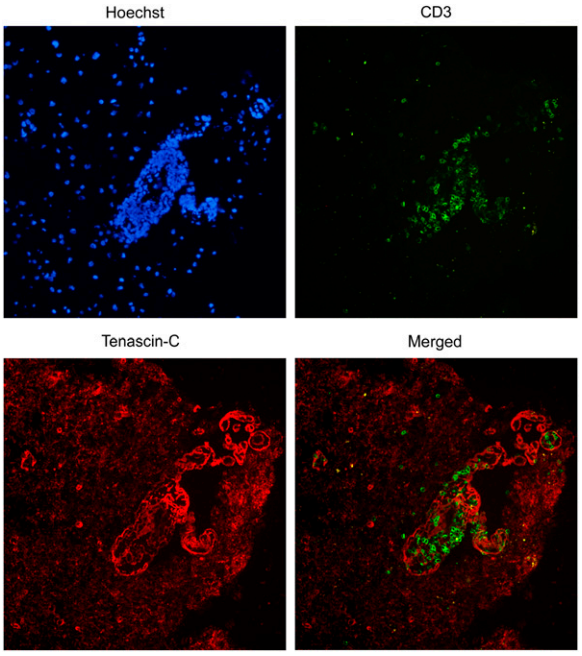

FIGURE 6. The expressions of tenascin-C and $CD3^+$ T cells in the glioma tissue. Five-micrometer serial tissue sections were prepared and mounted on slides. After blocking with PBS containing 10% FBS, the slides were incubated overnight at 4°C with a mouse anti-human tenascin-C mAb and a goat polyclonal anti-human CD3 Ab. Secondary incubation was done with anti-mouse secondary Ab (Alexa Fluor 594 conjugated) and anti-goat Ab (Alexa Fluor 488 conjugated). Cell nuclei were stained with Hoechst 33258. Signals from CD3 and tenascin-C were merged. Stained cells were observed with a fluorescent microscope.

To evaluate the requirement of kinases for the transmigration of Jurkat cells through the tumor cell monolayers, we inhibited ERK, PI3K, and PKA activities with U0126, LY294002, and H-89, respectively (Fig. 7*C*). The transmigration of Jurkat cells through the MCF-7 cell monolayer was reduced to 40% of the control by U0126, 50% by LY294002, and 50% by H-89. Inhibiting ERK and PI3K had few effects on the transmigration of Jurkat cells through the U-118MG cell monolayer. In addition, in the presence of U0126, the amount of amoeba-like Jurkat cells on the MCF-7 matrix was reduced by at least 30%, and round cells increased 2-fold. U0126 also slightly reduced the amount of rough Jurkat cells on the U-118MG matrix (Fig. 7*D*).

Because suppression of tenascin-C converts U-118MG cells to a transmigration-permissive phenotype, we hypothesized that ERK is the target kinase affected by tenascin-C (Fig. 8*A*). Jurkat cells in contact with the U-118MG (TNCshRNA) monolayer showed a higher level of ERK phosphorylation as compared with that in Jurkat cells on the control U-118MG. Because the chemotaxis-associated signaling molecules are spatially regulated and asymmetrically distributed in polarized migrating cells (30, 31), we examined the intracellular localization of ERK in Jurkat cells. Confocal images showed that the actin of Jurkat cells was partially colocalized with phosphorylated ERK at the leading edge when they were attached onto the ECM of U-118MG (TNCshRNA) (Fig. 8*B*). The conclusion scheme for the inhibition of T cell migration by tumor tenascin-C is shown in Fig. 9.

Discussion

Infiltration of T lymphocytes into tumor masses is critical for successful antitumor immune surveillance, which is positively

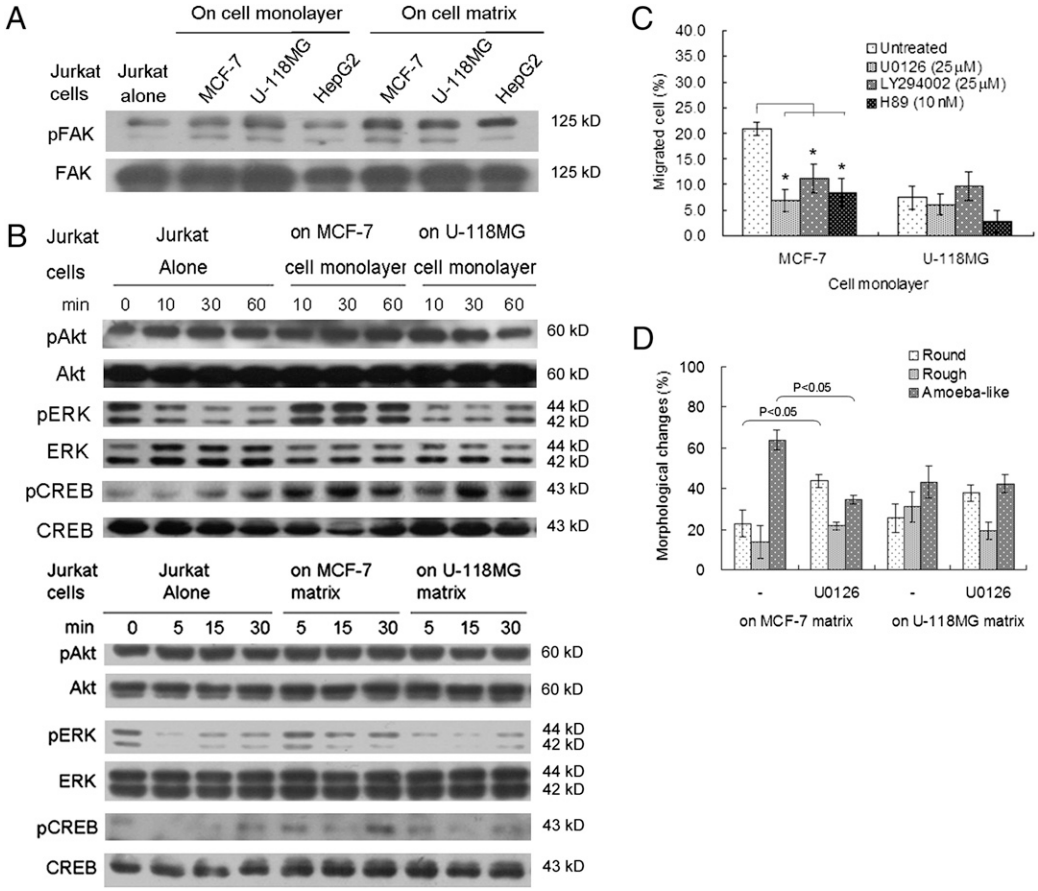

FIGURE 7. FAK, ERK, PI3K, and PKA kinases activity are required for the transmigration of Jurkat cells. Jurkat cells were added on the tumor ECM or cell monolayer and harvested at the indicated time points. *A*, FAK and pFAK of Jurkat cells containing 1% FBS/RPMI 1640 exposed to tumor cell monolayers or ECM for 10 min. *B*, Total proteins were extracted and subjected to Western blot analysis for ERK, pERK, AKT, pAKT, CREB, and pCREB. *C*, Jurkat cells were pretreated with U0126 (25 μM), LY294002 (25 μM), or H89 (10 μM) in 1% FBS/RPMI 1640 for 30 min. Cells transmigrated through tumor cell monolayers in a transwell unit were counted at 4 h. *D*, The morphological changes of Jurkat cells treated with or without U0126 (25 μM) were observed for 1 h using time-lapse microscopy. The mean ± SEM obtained from three independent experiments is shown. $*p < 0.05$. pAKT, phosphorylated AKT; pCREB; phosphorylated CREB; pERK, phosphorylated ERK.

correlated with better survival. In this study, we found that human leukemia T cell lines and primary T cells showed markedly low migration rates across monolayers or ECM of glioblastoma cells as compared with those of MCF-7 and HepG2. The low migration rate across glioblastoma cell monolayers is unlikely to be due to strong adhesion between Jurkat and glioblastoma cells, which potentially restrains cell motility by physical force. Jurkat cells were able to

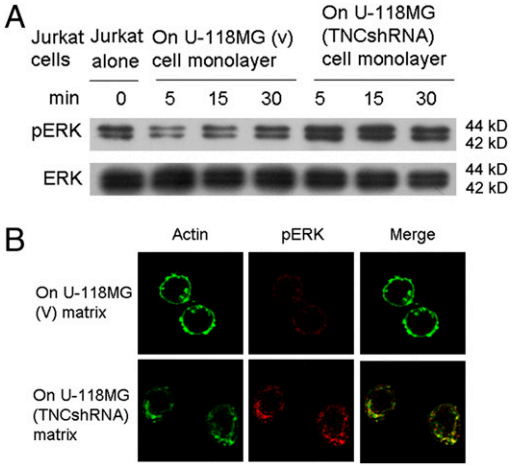

FIGURE 8. The expression and location of pERK of Jurkat cells adhered to the monolayer or ECM of U-118MG–derived cells. *A*, ERK phosphorylation of Jurkat cells on a monolayer of U-118MG–derived cells. *B*, After Jurkat cells were plated on tumor cell matrix for 1 h, pERK and actin were observed using confocal microscopy.

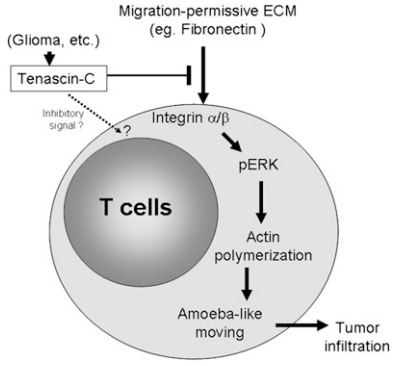

FIGURE 9. Scheme for the inhibition of T cell migration by tumor tenascin-C. Migration-permissive ECM, such as fibronectin, engages the integrin α/β of T cells to activate ERK, resulting in elevated actin polymerization and amoeba-like moving. This process will facilitate T cell infiltration into the tumor area. Tenascin-C secreted by glioblastoma to tumor stroma interferes the interaction of ECM and integrin that would blunt T cell migration.

adhere firmly onto HepG2, but still showed a high transmigration rate, indicating that the regulation for cell motility of T cells in tumor sites appears to be different than that for adhesion.

ECM extracted from tumors had similar effects as those of living cells. Using Abs or RGD peptide to block β1- and β2-integrin activation suppressed the transmigration rate of Jurkat cells, suggesting integrin-ECM interaction mediated this migration process. Blocking of α5β1 integrins reverses the inhibitory effect of tenascin-C on chemotaxis of human monocytes and neutrophils (28); however, the real receptor for effective tenascin-C binding is yet to be confirmed. Although Ab (BC-24) recognized an epitope located within the N-terminal EGF-like sequence of the human tenascin-C molecule and reduced the migration and proliferation of glioma cells (29), it reduced cell adhesion (32) but did not affect the transmigration rate of T cells through glioma cell monolayers (this study). It is thus possible that cell adhesion requires the EGFL domain but migration is blocked by other parts of tenascin-C.

By analyzing the ECM constituents of tumor cells, we detected fibronectin and laminin-γ1 at various levels. Notably, only glioblastoma cells expressed collagen IV and tenascin-C. Tenascin-C is highly expressed during embryogenesis but is downregulated in most adult tissues except for wound-healing regions and tumors (33). Recently, tenascin-C was identified as a prognostic marker for tumor recurrence and shown to play a role in glioblastoma growth and invasion (29). Tenascin-C inhibits β1-integrin–dependent T lymphocyte adhesion to fibronectin (34) and thus potentially inhibits the transmigration processes of Jurkat cells across glioblastoma cells. This speculation is supported by the finding that suppression of tenascin-C in glioma cells using the shRNA technique enhanced the transmigration rate of Jurkat cells and CD3/CD28-activated T cells in our transwell assay. Accordingly, adding human tenascin-C protein to MCF-7 and HepG2 effectively reduced the transmigration rate. (Figs. 3*B*, *lower panels*, 4*A*). Furthermore, $CD3^+$ T cells were mostly located in the boundary area that stained strongly for tenascin-C in glioma tissue (Fig. 7). Our result is consistent with a finding made in a tenascin-C knockout mouse model that spontaneously develops mammary tumors, in which enhanced infiltration of immune cells was detected in the tumor stroma of tenascin-C-null mice (35).

To understand the mechanism by which ECM of glioblastoma cells prevented the transmigration of Jurkat cells, we investigated the cell morphology and localization of F-actin. The low migration rate of Jurkat cells and plating on the tumor cell monolayer and matrix is consistent with reduced lamellipodia formation and F-actin polymerization at the leading front. Jurkat cells did not spread out well on the ECM of glioblastoma cells, but instead formed short podia-like protrusions that retracted frequently. In contrast, Jurkat cells can move around on ECM from U-118MG (TNCshRNA), further highlighting the pivotal role of tenascin-C on lymphocyte migration.

By analyzing the activation status and localization of migration-controlling kinases, we found that delayed ERK phosphorylation in Jurkat cells contacting U-118MG cells was associated with tenascin-C expression. Impairing transmigration by U0126 further demonstrated the requirement of ERK activity. In addition, Jurkat cells that went through the tumor monolayer in the transwell experiment always had higher ERK phosphorylation (data not shown). Jurkat cells are defective in phosphatase and tensin homologue deleted on chromosome 10, which antagonizes PI3K signaling by dephosphorylating phosphatidylinositol 3,4,5-trisphosphate (36). We detected consistently high AKT phosphorylation in Jurkat cells. Although blocking PKA and PI3K activities reduced the transmigration of Jurkat cells, we did not observe different inductions of these two kinases in Jurkat cells by contact with transmigration-permissive or nonpermissive tumor cells. It is likely that PKA and PI3K are important components of the migration machine but are controlled separately by other integrin signals. Migration-controlling kinases recruited to the leading front of migrating lymphocytes can facilitate actin polymerization (17, 18, 37). In agreement with these findings, the confocal images showed that phosphorylated ERK partly colocalized with actin on the leading edge of Jurkat cells. A higher migration of Jurkat cells on the matrix of U-118MG (TNCshRNA) was correlated with more phosphorylated ERK appearing on the leading edge.

It has been reported that brain tumor cells plated onto a mixed fibronectin/tenascin-C substratum fail to spread, accompanied by a lack of general FAK phosphorylation and autophosphorylation of FAK at Tyr-397 (38, 39). Tenascin-C not only interacts with other ECM molecules, such as perlecan and fibronectin, but also cell-surface receptors including integrins α2β1, αvβ3 and α9β1, annexin II, and syndecan (40). It is proposed that the inhibition of syndecan-4, Rho, and FAK in cell spreading and the fibronectin matrix assembly by tenascin-C are major mechanisms for cell detachment operating in solid tumors (41, 42). However, T lymphocytes express little syndecan-4 (43, 44). In addition, Jurkat cells, despite being defective in migration, showed normal phosphorylation of FAK when making contact with glioblastoma cells (Fig. 6*A*). Obviously, the integrin signals for lymphocyte trafficking are different from those for the migration of solid tumors.

In summary, tenascin-C expression of glioblastomas paralyzes T cell migration (Fig. 9), supporting the idea that some types of tumors may suppress local immune function by using ECMs to impair lymphocyte infiltration. Our findings provide a plausible explanation at the molecular level to explain why $CD3^+$ T lymphocytes were less frequently observed in glioma tumor nodules but scattered throughout the parenchyma (45, 46). Understanding the mechanisms of lymphocyte migration and how they are modulated by a tumor matrix will illuminate new targets for boosting immune surveillance against tumors.

Acknowledgments

We thank the National Core Facilities of the National Research Program for Genomic Medicine-Tumor Tissue Bank in Southern Taiwan for support.

Disclosures

The authors have no financial conflicts of interest.

References

1. Curiel, T. J., G. Coukos, L. Zou, X. Alvarez, P. Cheng, P. Mottram, M. Evdemon-Hogan, J. R. Conejo-Garcia, L. Zhang, M. Burow, et al. 2004. Specific recruitment of regulatory T cells in ovarian carcinoma fosters immune privilege and predicts reduced survival. *Nat. Med.* 10: 942–949.
2. Hiraoka, K., M. Miyamoto, Y. Cho, M. Suzuoki, T. Oshikiri, Y. Nakakubo, T. Itoh, T. Ohbuchi, S. Kondo, and H. Katoh. 2006. Concurrent infiltration by CD8+ T cells and CD4+ T cells is a favourable prognostic factor in non-small-cell lung carcinoma. *Br. J. Cancer* 94: 275–280.
3. Liakou, C. I., S. Narayanan, D. Ng Tang, C. J. Logothetis, and P. Sharma. 2007. Focus on TILs: Prognostic significance of tumor infiltrating lymphocytes in human bladder cancer. *Cancer Immun.* 7: 10–16.
4. Schumacher, K., W. Haensch, C. Röefzaad, and P. M. Schlag. 2001. Prognostic significance of activated CD8(+) T cell infiltrations within esophageal carcinomas. *Cancer Res.* 61: 3932–3936.
5. Galon, J., A. Costes, F. Sanchez-Cabo, A. Kirilovsky, B. Mlecnik, C. Lagorce-Pagès, M. Tosolini, M. Camus, A. Berger, P. Wind, et al. 2006. Type, density, and location of immune cells within human colorectal tumors predict clinical outcome. *Science* 313: 1960–1964.
6. Zhang, L., J. R. Conejo-Garcia, D. Katsaros, P. A. Gimotty, M. Massobrio, G. Regnani, A. Makrigiannakis, H. Gray, K. Schlienger, M. N. Liebman, et al. 2003. Intratumoral T cells, recurrence, and survival in epithelial ovarian cancer. *N. Engl. J. Med.* 348: 203–213.
7. Reddig, P. J., and R. L. Juliano. 2005. Clinging to life: cell to matrix adhesion and cell survival. *Cancer Metastasis Rev.* 24: 425–439.
8. Hehlgans, S., M. Haase, and N. Cordes. 2007. Signalling via integrins: implications for cell survival and anticancer strategies. *Biochim. Biophys. Acta* 1775: 163–180.

9. Su, C. C., Y. P. Lin, Y. J. Cheng, J. Y. Huang, W. J. Chuang, Y. S. Shan, and B. C. Yang. 2007. Phosphatidylinositol 3-kinase/Akt activation by integrin-tumor matrix interaction suppresses Fas-mediated apoptosis in T cells. *J. Immunol.* 179: 4589–4597.
10. Górski, A., J. Piekarczyk, H. Skurzak, M. Nowaczyk, B. Dybowska, B. Stepień-Sopniewska, G. Korczak-Kowalska, J. Pazdur, and A. Filipowicz-Sosnowska. 1993. Abnormalities in T cell interactions with the extracellular matrix proteins in a patient with Wegener's granulomatosis. *Clin. Immunol. Immunopathol.* 69: 149–154.
11. Torimura, T., T. Ueno, S. Inuzuka, M. Tanaka, H. Abe, and K. Tanikawa. 1991. Mechanism of fibrous capsule formation surrounding hepatocellular carcinoma. Immunohistochemical study. *Arch. Pathol. Lab. Med.* 115: 365–371.
12. Menon, A. G., G. J. Fleuren, E. A. Alphenaar, L. E. Jonges, C. M. Janssen van Rhijn, N. G. Ensink, H. Putter, R. A. Tollenaar, C. J. van de Velde, and P. J. Kuppen. 2003. A basal membrane-like structure surrounding tumour nodules may prevent intraepithelial leucocyte infiltration in colorectal cancer. *Cancer Immunol. Immunother.* 52: 121–126.
13. Schaumburg-Lever, G., I. Lever, B. Fehrenbacher, H. Möller, B. Bischof, E. Kaiserling, C. Garbe, and G. Rassner. 2000. Melanocytes in nevi and melanomas synthesize basement membrane and basement membrane-like material. An immunohistochemical and electron microscopic study including immunoelectron microscopy. *J. Cutan. Pathol.* 27: 67–75.
14. Ratner, S. 1992. Lymphocyte migration through extracellular matrix. *Invasion Metastasis* 12: 82–100.
15. Yang, Q., S. Goding, M. Hagenaars, T. Carlos, P. Albertsson, P. Kuppen, U. Nannmark, M. E. Hokland, and P. H. Basse. 2006. Morphological appearance, content of extracellular matrix and vascular density of lung metastases predicts permissiveness to infiltration by adoptively transferred natural killer and T cells. *Cancer Immunol. Immunother.* 55: 699–707.
16. Edwards, S., P. F. Lalor, C. Tuncer, and D. H. Adams. 2006. Vitronectin in human hepatic tumours contributes to the recruitment of lymphocytes in an alpha v beta3-independent manner. *Br. J. Cancer* 95: 1545–1554.
17. Rickert, P., O. D. Weiner, F. Wang, H. R. Bourne, and G. Servant. 2000. Leukocytes navigate by compass: roles of PI3Kgamma and its lipid products. *Trends Cell Biol.* 10: 466–473.
18. Srinivasan, S., F. Wang, S. Glavas, A. Ott, F. Hofmann, K. Aktories, D. Kalman, and H. R. Bourne. 2003. Rac and Cdc42 play distinct roles in regulating PI (3,4,5)P3 and polarity during neutrophil chemotaxis. *J. Cell Biol.* 160: 375–385.
19. Howe, A. K., and R. L. Juliano. 2000. Regulation of anchorage-dependent signal transduction by protein kinase A and p21-activated kinase. *Nat. Cell Biol.* 2: 593–600.
20. Hecht, I., L. Cahalon, R. Hershkoviz, A. Lahat, S. Franitza, and O. Lider. 2003. Heterologous desensitization of T cell functions by CCR5 and CXCR4 ligands: inhibition of cellular signaling, adhesion and chemotaxis. *Int. Immunol.* 15: 29–38.
21. Woods, M. L., and Y. Shimizu. 2001. Signaling networks regulating beta1 integrin-mediated adhesion of T lymphocytes to extracellular matrix. *J. Leukoc. Biol.* 69: 874–880.
22. Giese, A., M. D. Rief, M. A. Loo, and M. E. Berens. 1994. Determinants of human astrocytoma migration. *Cancer Res.* 54: 3897–3904.
23. Kim, S. J., J. H. Park, J. E. Lee, J. M. Kim, J. B. Lee, S. Y. Moon, S. I. Roh, C. G. Kim, and H. S. Yoon. 2004. Effects of type IV collagen and laminin on the cryopreservation of human embryonic stem cells. [Published retraction appears in 2006. *Stem Cells* 24: 804.] *Stem Cells* 22: 950–961.
24. Kikkawa, Y., N. Sanzen, and K. Sekiguchi. 1998. Isolation and characterization of laminin-10/11 secreted by human lung carcinoma cells. laminin-10/11 mediates cell adhesion through integrin alpha3 beta1. *J. Biol. Chem.* 273: 15854–15859.
25. Mighell, A. J., J. Thompson, W. J. Hume, A. F. Markham, and P. A. Robinson. 1997. Human tenascin-C: identification of a novel type III repeat in oral cancer and of novel splice variants in normal, malignant and reactive oral mucosae. *Int. J. Cancer* 72: 236–240.
26. Baratelli, F., Y. Lin, L. Zhu, S. C. Yang, N. Heuzé-Vourc'h, G. Zeng, K. Reckamp, M. Dohadwala, S. Sharma, and S. M. Dubinett. 2005. Prostaglandin E2 induces FOXP3 gene expression and T regulatory cell function in human CD4+ T cells. *J. Immunol.* 175: 1483–1490.
27. Kuznetsova, S. A., and D. D. Roberts. 2004. Functional regulation of T lymphocytes by modulatory extracellular matrix proteins. *Int. J. Biochem. Cell Biol.* 36: 1126–1134.
28. Loike, J. D., L. Cao, S. Budhu, S. Hoffman, and S. C. Silverstein. 2001. Blockade of alpha 5 beta 1 integrins reverses the inhibitory effect of tenascin on chemotaxis of human monocytes and polymorphonuclear leukocytes through three-dimensional gels of extracellular matrix proteins. *J. Immunol.* 166: 7534–7542.
29. Herold-Mende, C., M. M. Mueller, M. M. Bonsanto, H. P. Schmitt, S. Kunze, and H. H. Steiner. 2002. Clinical impact and functional aspects of tenascin-C expression during glioma progression. *Int. J. Cancer* 98: 362–369.
30. Servant, G., O. D. Weiner, P. Herzmark, T. Balla, J. W. Sedat, and H. R. Bourne. 2000. Polarization of chemoattractant receptor signaling during neutrophil chemotaxis. *Science* 287: 1037–1040.
31. Franca-Koh, J., and P. N. Devreotes. 2004. Moving forward: mechanisms of chemoattractant gradient sensing. *Physiology (Bethesda)* 19: 300–308.
32. Fischer, D., M. Brown-Lüdi, T. Schulthess, and R. Chiquet-Ehrismann. 1997. Concerted action of tenascin-C domains in cell adhesion, anti-adhesion and promotion of neurite outgrowth. *J. Cell Sci.* 110: 1513–1522.
33. Orend, G. 2005. Potential oncogenic action of tenascin-C in tumorigenesis. *Int. J. Biochem. Cell Biol.* 37: 1066–1083.
34. Hauzenberger, D., P. Olivier, D. Gundersen, and C. Rüegg. 1999. Tenascin-C inhibits beta1 integrin-dependent T lymphocyte adhesion to fibronectin through the binding of its fnIII 1-5 repeats to fibronectin. *Eur. J. Immunol.* 29: 1435–1447.
35. Mackie, E. J., and R. P. Tucker. 1999. The tenascin-C knockout revisited. *J. Cell Sci.* 112: 3847–3853.
36. Shan, X., M. J. Czar, S. C. Bunnell, P. Liu, Y. Liu, P. L. Schwartzberg, and R. L. Wange. 2000. Deficiency of PTEN in Jurkat T cells causes constitutive localization of Itk to the plasma membrane and hyperresponsiveness to CD3 stimulation. *Mol. Cell. Biol.* 20: 6945–6957.
37. Lorenowicz, M. J., M. Fernandez-Borja, and P. L. Hordijk. 2007. cAMP signaling in leukocyte transendothelial migration. *Arterioscler. Thromb. Vasc. Biol.* 27: 1014–1022.
38. Huang, W., R. Chiquet-Ehrismann, J. V. Moyano, A. Garcia-Pardo, and G. Orend. 2001. Interference of tenascin-C with syndecan-4 binding to fibronectin blocks cell adhesion and stimulates tumor cell proliferation. *Cancer Res.* 61: 8586–8594.
39. Orend, G., W. Huang, M. A. Olayioye, N. E. Hynes, and R. Chiquet-Ehrismann. 2003. Tenascin-C blocks cell-cycle progression of anchorage-dependent fibroblasts on fibronectin through inhibition of syndecan-4. *Oncogene* 22: 3917–3926.
40. Chiquet-Ehrismann, R., and M. Chiquet. 2003. Tenascins: regulation and putative functions during pathological stress. *J. Pathol.* 200: 488–499.
41. Midwood, K. S., and J. E. Schwarzbauer. 2002. Tenascin-C modulates matrix contraction via focal adhesion kinase- and Rho-mediated signaling pathways. *Mol. Biol. Cell* 13: 3601–3613.
42. Wierzbicka-Patynowski, I., and J. E. Schwarzbauer. 2003. The ins and outs of fibronectin matrix assembly. *J. Cell Sci.* 116: 3269–3276.
43. Kaneider, N. C., C. M. Reinisch, S. Dunzendorfer, J. Römisch, C. J. Wiedermann, and C. J. Wiederman. 2002. Syndecan-4 mediates antithrombin-induced chemotaxis of human peripheral blood lymphocytes and monocytes. [Published erratum appears in 2002. *J. Cell Sci.* 115: 454.] *J. Cell Sci.* 115: 227–236.
44. Yamashita, Y., K. Oritani, E. K. Miyoshi, R. Wall, M. Bernfield, and P. W. Kincade. 1999. Syndecan-4 is expressed by B lineage lymphocytes and can transmit a signal for formation of dendritic processes. *J. Immunol.* 162: 5940–5948.
45. Giometto, B., F. Bozza, F. Faresin, L. Alessio, S. Mingrino, and B. Tavolato. 1996. Immune infiltrates and cytokines in gliomas. *Acta Neurochir. (Wien)* 138: 50–56.
46. Walker, D. G., T. Chuah, M. J. Rist, and M. P. Pender. 2006. T-cell apoptosis in human glioblastoma multiforme: implications for immunotherapy. *J. Neuroimmunol.* 175: 59–68.